Xuqing Chen,[1,2] Feifei Zhang,[1] Qi Gong,[1] Aoyuan Cui,[1] Shu Zhuo,[1] Zhimin Hu,[1] Yamei Han,[1] Jing Gao,[1] Yixuan Sun,[3] Zhengshuai Liu,[1] Zhongnan Yang,[2] Yingying Le,[1] Xianfu Gao,[4] Lily Q. Dong,[5] Xin Gao,[3] and Yu Li[1]

Hepatic ATF6 Increases Fatty Acid Oxidation to Attenuate Hepatic Steatosis in Mice Through Peroxisome Proliferator–Activated Receptor α

Diabetes 2016;65:1904–1915 | DOI: 10.2337/db15-1637

SIGNAL TRANSDUCTION

The endoplasmic reticulum quality control protein activating transcription factor 6 (ATF6) has emerged as a novel metabolic regulator. Here, we show that adenovirus-mediated overexpression of the dominant-negative form of ATF6 (dnATF6) increases susceptibility to develop hepatic steatosis in diet-induced insulin-resistant mice and fasted mice. Overexpression of dnATF6 or small interfering RNA–mediated knockdown of ATF6 decreases the transcriptional activity of peroxisome proliferator–activated receptor α (PPARα)/retinoid X receptor complex, and inhibits oxygen consumption rates in hepatocytes, possibly through inhibition of the binding of PPARα to the promoter of its target gene. Intriguingly, ATF6 physically interacts with PPARα, enhances the transcriptional activity of PPARα, and triggers activation of PPARα downstream targets, such as CPT1α and MCAD, in hepatocytes. Furthermore, hepatic overexpression of the active form of ATF6 promotes hepatic fatty acid oxidation and protects against hepatic steatosis in diet-induced insulin-resistant mice. These data delineate the mechanism by which ATF6 controls the activity of PPARα and hepatic mitochondria fatty acid oxidation. Therefore, strategies to activate ATF6 could be used as an alternative avenue to improve liver function and treat hepatic steatosis in obesity.

Hepatic fatty acid oxidation is one of the central processes in hepatic lipid metabolism. The inability of fatty acid to be adequately oxidized causes aberrant accumulation of triglyceride in the liver and results in the development of hepatic steatosis or nonalcoholic fatty liver disease. Hepatic steatosis is one of the most common and potentially serious metabolic diseases, which can progress to nonalcoholic steatohepatitis, cirrhosis, and liver cancer (1,2).

The unfolded protein response (UPR) is induced by the endoplasmic reticulum (ER) stress to attenuate protein synthesis, increase protein folding, and enhance activity of degradation pathways in the ER (2). There are three well-characterized proximal ER-resident sensors of the UPR: activating transcription factor 6 (ATF6), protein kinase-like ER kinase (PERK), and kinase and endoribonuclease inositol-requiring enzyme 1 (IRE1) (3,4). ATF6 translocates to the Golgi, where it is cleaved by the site 1 and site 2 proteases to release the soluble N-terminal fragment, which translocates to the nucleus to activate expression of a spectrum of UPR mediators. PERK-induced phosphorylation of eukaryotic initiation factor 2α blocks global protein translation. IRE1 initiates an unconventional mRNA splicing of X-box binding protein 1 (XBP1) to produce an active transcription factor (3,4). The UPR plays an important role in metabolic diseases such as type 2 diabetes, insulin resistance, and obesity (5,6).

ATF6 is a key regulator of ER quality control protein in mammalian cells (7). Recently, ATF6 has been revealed as a critical regulator to improve metabolic functions in mice. ATF6 inhibits hepatic gluconeogenesis by disrupting

[1]Key Laboratory of Nutrition and Metabolism, Institute for Nutritional Sciences, Shanghai Institutes for Biological Sciences, Chinese Academy of Sciences, University of Chinese Academy of Sciences, Shanghai, China
[2]College of Life and Environmental Sciences, Shanghai Normal University, Shanghai, China
[3]Department of Endocrinology and Metabolism, Zhongshan Hospital, Fudan University, Shanghai, China
[4]Key Laboratory of Systems Biology, Institute of Biochemistry and Cell Biology, Shanghai Institutes for Biological Sciences, Chinese Academy of Sciences, Shanghai, China
[5]Department of Cellular and Structural Biology, University of Texas Health Science Center at San Antonio, San Antonio, TX
Corresponding author: Yu Li, liyu@sibs.ac.cn.

Received 30 November 2015 and accepted 6 April 2016.
This article contains Supplementary Data online at http://diabetes.diabetesjournals.org/lookup/suppl/doi:10.2337/db15-1637/-/DC1.

the CREB-CRTC2 interaction and thereby improving glucose metabolism (8). ATF6 improves skeletal muscle function and provides metabolic benefits through interacting with PGC1α (9). ATF6 mediates thrombospondin-induced protection of myocardial injury (10). Moreover, activation of ATF6 mediates vascular endothelial growth factor–induced endothelial cell survival and angiogenesis (11). ATF6's target XBP1 inhibits gluconeogenesis in genetic and diet-induced obesity (12). Intriguingly, whole-body ATF6α-knockout (KO) mice show exacerbated diet-induced hepatic steatosis and glucose intolerance (13) and are susceptible to develop hepatic steatosis in response to the ER stress inducer tunicamycin (14,15). However, whether and how hepatic ATF6 deficiency affects hepatic lipid metabolism in response to dietary overloading remain largely unknown.

Peroxisome proliferator–activated receptor α (PPARα) is a key transcriptional factor and plays essential roles in the regulation of hepatic fatty acid oxidation and subsequent ketogenesis. PPARα is predominantly expressed in the liver. PPARα forms heterodimers with the retinoid X receptor (RXR), activates the transcription of a family of genes containing a PPAR response element (PPRE), and regulates lipid homeostasis in response to nutrient availability (16). PPARα-KO mice exhibit hepatic steatosis in response to fasting due to decreased levels of fatty acid oxidation and ketogenesis (17). However, the mechanisms in regulating the transcriptional activity of PPARα during diet-induced obesity and the adaptive fasting response remain incompletely understood.

In this study we show that hepatic ATF6-inhibited mice are prone to hepatic steatosis with reduced fatty acid oxidation. Gain- and loss-of-function studies in livers and in hepatocytes identify ATF6 as an important transcriptional regulator of hepatic fat metabolism and provide insight into the mechanism by which ATF6 controls hepatic fatty acid oxidation through coactivation of PPARα.

RESEARCH DESIGN AND METHODS

Animal Model and Diets

Male C57BL/6 mice were purchased from Shanghai Laboratory Animal Co. Ltd., Shanghai, China. Mice were fed a high-fat, high-sucrose (HFHS) diet (D12327; Research Diets) for 12 weeks, followed by treatment with adenoviruses encoding a nuclear active form of ATF6 (Ad-nATF6), a dominant-negative mutant of ATF6 (Ad-dnATF6), or green fluorescent protein (Ad-GFP) via tail vein injection. All mice were housed under a 12:12-h light/dark cycle at controlled temperature. All animal experimental protocols were approved by the Institute for Nutritional Sciences Institutional Animal Care and Use Committee, Shanghai Institutes for Biological Sciences, Chinese Academy of Sciences.

Liver Histological Analysis

Livers were fixed in 10% phosphate-buffered formalin acetate at 4°C overnight and embedded in paraffin wax. Paraffin sections (5 μm) were cut and mounted on glass slides for hematoxylin and eosin (H&E) staining, as previously described (18,19). Livers embedded in optimum cutting temperature compound (Tissue-Tek; Laborimpex) were used for Oil Red O staining for the assessment of hepatic steatosis according to the manufacturer's instructions (American MasterTech, Lodi, CA).

Body Composition Analysis

Body composition was determined with the nuclear magnetic resonance system using a Body Composition Analyzer MiniQMR23-060H-I (Niumag, China). Body fat, lean mass, body fluids, and total body water were measured in live conscious mice with ad libitum access to diet, as described previously (20).

Plasmid Construction and Transfection

The expression plasmids encoding a soluble and active form of ATF6 (nATF6) or a dominant-negative mutant of ATF6 (dnATF6) that contains DNA-binding and dimerization domains but lacking an activation domain were constructed by PCR-mediated amplification of the regions corresponding to amino acids 1 to 373 or 171 to 373 of human ATF6, respectively, as described previously (21), followed by subcloning into the *Hin*dIII/*Xba*I sites of a shuttle vector (pShuttle-CMV), respectively. The *myc* epitope tag was fused in frame to the 5′ terminus of the coding sequence. The plasmid expressing glutathione S-transferase (GST)-tagged human nATF6 (GST-nATF6) was constructed by cloning the human ATF6 cDNA encoding amino acids 1 to 373 into the *Cla*I/*Not*I sites of pEBG (a GST fusion vector). The plasmids encoding pSG5-PPARα (22) and Sport-RXRα (22) were purchased from Addgene (Cambridge, MA). Transfection assays for plasmids were performed using Lipofectamine 2000 (Life Technologies) according to the manufacturer's protocol.

Dual Luciferase Activity Assays

Dual luciferase assays were performed as described previously (18). Luciferase activity was measured using an Infinite 200 PRO plate reader (Tecan, Männedorf, Switzerland). The firefly luciferase activity was normalized to the *Renilla* luciferase activity (*firefly* luciferase/*Renilla* luciferase) and presented as relative luciferase activity.

RNA Isolation and Quantitative RT-PCR Analysis

Liver tissues were homogenized in TRIzol Reagent (Life Technologies), and total RNAs were reversely transcribed to cDNA using SuperScript II reverse transcriptase (Life Technologies) and Oligo d (T). The resulting cDNA was subjected to real-time PCR with gene-specific primers in the presence of SYBR Green PCR Master Mix (Applied Biosystems) using the StepOnePlus Real-Time PCR System (Applied Biosystems), as described previously (23).

In Vivo Adenoviral Gene Transfer

Adenovirus-mediated gene transfer of Ad-nATF6, Ad-dnATF6, or Ad-GFP in the liver of C57BL/6 mice was

accomplished as described previously (20,24,25). Adenoviruses (5×10^9 plaque-forming units, $\sim 1 \times 10^{10}$ plaque-forming units per mouse) were delivered into mice by tail vein injection. Two weeks postinjection, mice were killed in a postprandial state under isoflurane anesthesia, and tissues were rapidly taken and freshly frozen in liquid nitrogen and then stored at −80°C or fixed for histologic analysis.

Statistical Analysis

Data are expressed as mean ± SEM. Statistical significance was evaluated using the unpaired two-tailed Student *t* test and among more than two groups by analysis of one-way ANOVA. Differences were considered significant at $P < 0.05$.

RESULTS

Hepatic Steatosis and Insulin Resistance Are Exacerbated in Hepatic ATF6-Inhibited Mice Fed the HFHS Diet

To investigate whether the key ER quality control protein ATF6 (7) is a driving force in maintaining hepatic lipid homeostasis, we developed a mouse model by adenovirus-mediated hepatic expression of a dominant-negative version of ATF6 (Ad-dnATF6) encoding amino acids 171 to 373 that contains DNA-binding and dimerization domains but lacks an activation domain (21,26). C57BL/6 mice were placed on a chow diet and 12 weeks on a type 2 diabetogenic diet composed of HFHS and then treated with Ad-dnATF6 or Ad-GFP via tail vein injection, respectively. Chow-fed Ad-dnATF6 mice did not show significant metabolic changes compared with Ad-GFP–treated mice (Fig. 1*A*–*C* and Supplementary Fig. 1*A*). However, inhibition of ATF6 by dnATF6 caused a significant induction of liver and plasma triglyceride levels, suggesting a critical role of hepatic ATF6 in mediating lipid metabolism. Consistently, increased hepatic steatosis in Ad-dnATF6–treated mice was evidenced by H&E and Oil Red O staining, suggesting impaired hepatic lipid metabolism, which is consistent with exacerbated hepatic steatosis in ATF6-KO mice under tunicamycin challenge (15). Notably, body weight and liver weight, and body composition of fat mass and lean mass were not obviously changed (Supplementary Fig. 1*A* and *B*).

We determined in vivo function of hepatic dnATF6 on glucose homeostasis and insulin sensitivity. Fasting plasma glucose, insulin concentrations, and the calculated value for the homeostasis model assessment of insulin resistance were significantly increased in dnATF6-expressing mice compared with those in GFP-treated mice (Fig. 1*D* and Supplementary Fig. 1*C*). The effects of hepatic dnATF6 on glucose homeostasis and insulin sensitivity were further demonstrated by intraperitoneal glucose and insulin tolerance tests. Adenovirus-mediated overexpression of dominant-negative form dnATF6 exacerbated HFHS diet–induced glucose intolerance and insulin resistance, supporting the essential role of hepatic ATF6 in mediating lipid and glucose metabolism (Fig. 1*E* and *F*).

Expression Levels of UPR Mediators and Hepatic Fatty Acid Oxidation Are Attenuated in Hepatic ATF6-Inhibited Mice Fed the HFHS Diet

We next delineated the mechanism underlying the steatotic and insulin resistant phenotypes observed in dnATF6-treated mice. The infection efficiency of dnATF6 was evidenced by RT-PCR using primers targeting the coding region of amino acids 171 to 373 of human ATF6 for specific detection of overexpressed dnATF6 (Fig. 2*A*). As shown in Fig. 2*B* and *C*, the effects of dnATF6 administration were further confirmed by reduced expression levels of UPR mediators such as GRP78, XBP1, EDEM, CHOP, and endogenous ATF6. These data indicate adenoviral overexpression of dnATF6 is sufficient to suppress the hepatic UPR response in the liver of mice fed the HFHS diet.

Recent study shows that the expression level of PPARα, a key transcriptional regulator of genes involved in β-oxidation, was reduced in ATF6-KO mouse livers under tunicamycin treatment (15), suggesting a possible mechanism of PPARα in mediating ATF6's regulation of liver metabolism. As shown in Fig. 2*D*, administration of Ad-dnATF6 significantly decreased expression of several PPARα downstream targets, such as MCAD, EHHADH, ACOX, CPT1α, Cyp4A10, Cyp4A14, and FGF21 (27). These results suggest that loss of hepatic ATF6 impairs PPARα-mediated fatty acid metabolism. Moreover, expression levels of key enzymes involved in ketogenesis, such as ACAT1, HMGCS2, and BDH1, were decreased, which resulted in a reduction of plasma β-hydroxybutyrate concentrations (Fig. 2*E* and *F*). Notably, the mRNA levels of the key genes involved in fatty acid and triglyceride biosynthesis, such as SREBP-1c and FAS, and cholesterol biosynthesis, such as HMGCS and HMGCR, were not obviously changed (Supplementary Fig. 2*A* and *B*), whereas ATF6 may be sufficient to maintain the expression of some SREBP-2 target genes, which is consistent with the previous study showing that ATF6 suppresses SREBP-2 in HepG2 cells at basal conditions (28). Taken together, it appears to suggest that hepatic inhibition of ATF6 exacerbates HFHS diet–induced hepatic steatosis, possibly through hepatic impairment of PPARα signaling and fatty acid oxidation.

ATF6 Is Sufficient to Enhance Hepatic Fatty Acid Oxidation In Vitro

To investigate the effects of nATF6 on the expression of PPARα target genes, the in vitro activity of nATF6 was determined by measuring the activities of ERSE-I and ERSE-II, the key *cis*-acting elements capable of binding to ATF6 (29). As shown in Fig. 3*A* and *B* and in Supplementary Fig. 3*A*, treatment with *myc*-tagged nATF6, a soluble and active form of ATF6 (21), caused a robust induction of transcriptional activity on the ERSE-I and ERSE-II luciferase reporters in HepG2 cells and HEK293T cells, suggesting that nATF6 is sufficient to promote the

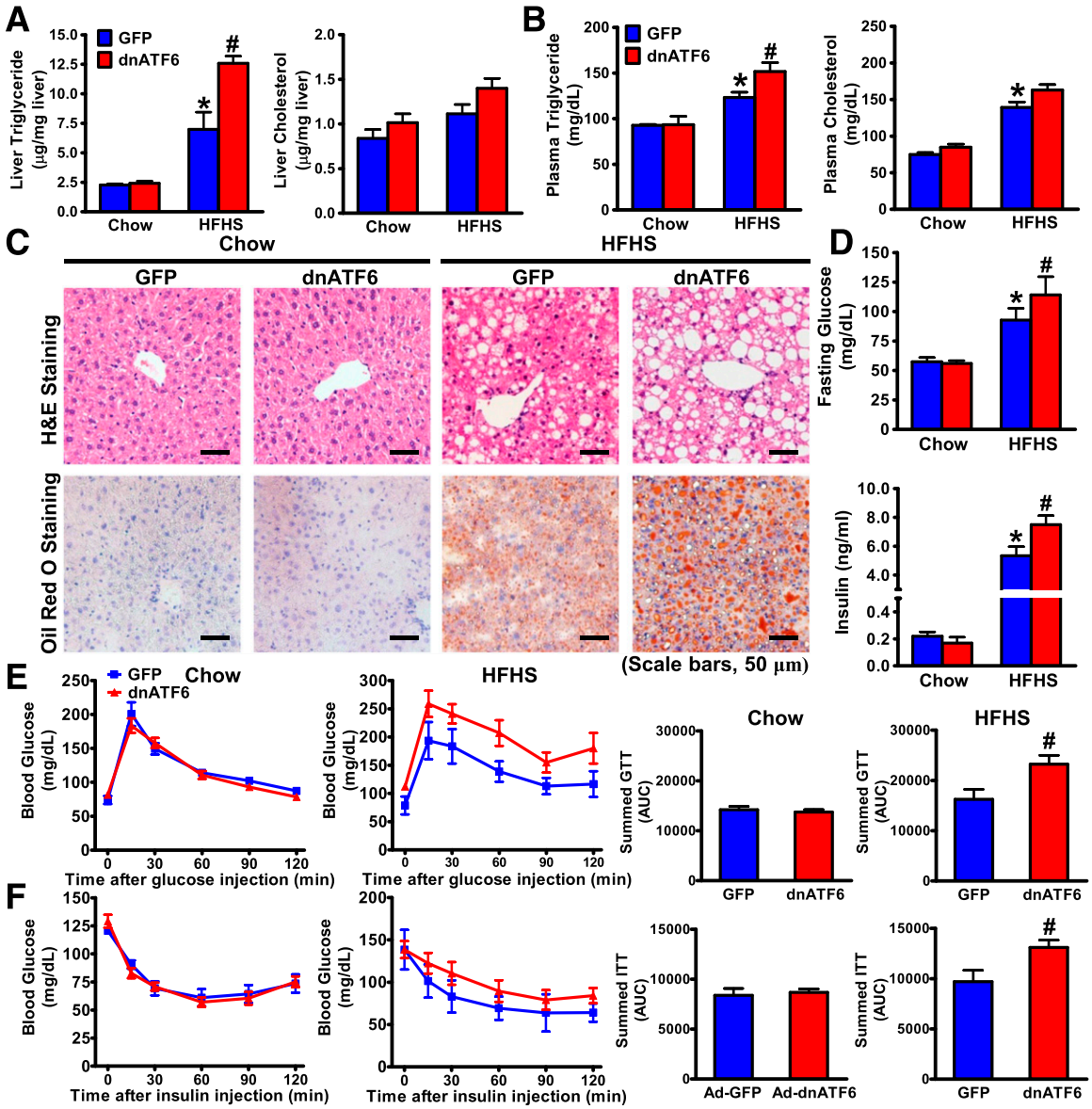

Figure 1—Adenovirus-mediated overexpression of dominant-negative ATF6 increases susceptibility to develop hepatic steatosis and insulin resistance in HFHS diet–fed mice. Male C57BL/6 mice (8 weeks old) were fed a chow diet for 2 weeks or an HFHS diet for 12 weeks, followed by treatment with Ad-GFP or Ad-dnATF6 via tail vein injection for 2 weeks. Inhibition of ATF6 increases hepatic steatosis in HFHS diet–fed mice. Liver (*A*) and plasma (*B*) triglyceride and cholesterol levels were assessed in mice. *C*: Representative H&E and Oil Red O staining are shown (scale bars: 50 μm). *D*: Blood glucose and plasma insulin levels were assessed. Glucose tolerance tests (GTTs) (1 g/kg) (*E*) or insulin tolerance tests (ITTs) (1 unit/kg) (*F*) were performed in mice after 16 h or 6 h of food deprivation 7 days or 9 days after the first injection of adenoviruses, respectively. AUC, area under the curve. The data are represented as the mean ± SEM (n = 5–7). *P < 0.05 vs. chow and Ad-GFP; #P < 0.05 vs. HFHS and Ad-GFP.

UPR response. Notably, overexpression of nATF6 was confirmed by immunoblots. Moreover, nATF6 increased expression levels of PPARα target genes, such as CPT1α and MCAD, in HepG2 cells (Fig. 3*C*). To demonstrate whether PPARα is required for the effects of ATF6 on hepatic fatty acid oxidation, 10 μmol/L PPARα antagonist GW6471, which was shown to specifically inhibit PPARα activity in rat liver cells (30,31), was used. Strikingly, nATF6-induced mRNA levels of CPT1α and MCAD were largely abrogated by treatment with GW6471 in HepG2 cells (Fig. 3*D*), suggesting a critical role of PPARα in ATF6-mediated fatty acid oxidation in vitro.

ATF6 Is Essential for PPARα to Regulate Hepatic Fatty Acid Oxidation In Vitro

Furthermore, to explore whether ATF6 is essential for the activation of UPR mediators in vitro, ATF6 loss-of-function approaches were assessed in hepatocytes. As shown in Fig. 4*A*, consistent with previous observations in HeLa cells (21), overexpression of dnATF6 potently blocked

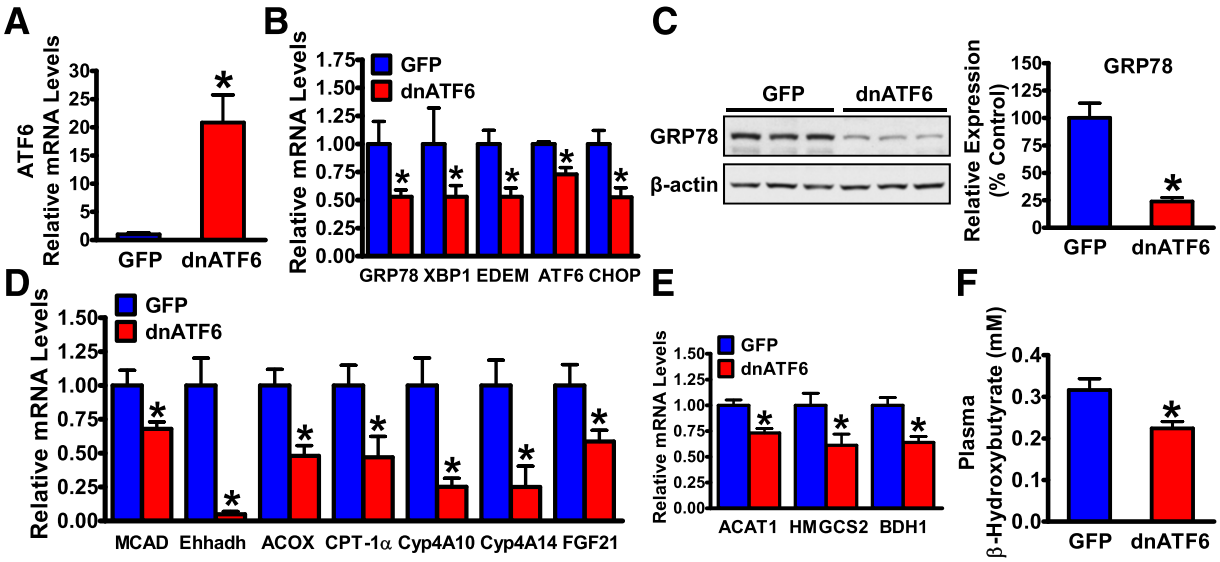

Figure 2—Hepatic overexpression of dnATF6 represses expression levels of UPR mediators and inhibits hepatic fatty acid oxidation in HFHS diet–fed mice. *A*: Hepatic expression of dnATF6 in mice fed the HFHS diet. PCR primers targeting the 171- to 373-amino acid–coding region of overexpressed human dnATF6 were used. Inhibition of ATF6 represses mRNA (*B*) and protein (*C*) levels of UPR mediators in livers of HFHS diet–fed mice. Hepatic gene expression of GRP78, XBP1, EDEM, CHOP, and endogenous ATF6 was determined by real-time PCR. Representative immunoblots and densitometric quantification for expression of GRP78 in the livers from three mice in each group are shown. Relative expression levels were normalized to β-actin. Hepatic fatty acid oxidation is abrogated by dnATF6 in HFHS diet–fed mice. The mRNA levels of PPARα targets (*D*) and key ketogenic enzymes (*E*) were measured. *F*: Plasma levels of β-hydroxybutyrate in mice. The data are represented as the mean ± SEM (n = 6–7). *$P < 0.05$ vs. HFHS and Ad-GFP.

thapsigargin-induced activation of ERSE-I and ERSE-II luciferase reporters, suggesting dnATF6 is sufficient to exhibit a dominant-negative effect on endogenous ATF6 activity. The effects of dnATF6 on expression of hepatic UPR genes were further assessed in HepG2 cells. Consistent with the results obtained in mouse livers in Fig. 2, administration of dnATF6 abrogated thapsigargin- or tunicamycin-induced expression of UPR mediators, such as GRP78, XBP1, and CHOP, suggesting that dnATF6 is a potent inhibitor of hepatic UPR (Fig. 4*B* and Supplementary Fig. 3*B*).

To determine whether ATF6 is required by PPARα to activate fatty acid oxidation, experiments were performed in HepG2 cells treated with the PPARα agonist WY14643. As shown in Fig. 4*C*, WY14643-stimulated induction of CPT1α and MCAD was attenuated by dnATF6. Consistently, knockdown of ATF6 by small interfering (si) RNAs in HepG2 cells resulted in a profound decrease in WY14643-stimulated fatty acid oxidation gene expression such as CPT-1α and MCAD (Fig. 4*D* and *E*). To investigate the functional consequence of inhibition of ATF6, cellular oxygen consumption rates, an index of mitochondrial oxidation function, were measured using the Seahorse Bioscience extracellular flux analyzer in HepG2 cells. Interestingly, as shown in Fig. 4*F*, the bioenergetics profiles and calculated oxygen consumption rates of cells treated with dnATF6 showed a significant decrease in basal and maximal mitochondrial respiratory capacity, consistent with the decreased CPT1α and MCAT expression observed in livers from mice fed the HFHS diet and HepG2 cells treated with dnATF6 (Figs. 2*D* and 4*C*). Taken together, these studies indicate that ATF6 is necessary for PPARα's activation of downstream signaling and improvement in hepatic fatty acid oxidation in vitro.

The Transcriptional Activity of PPARα Is in an ATF6-Dependent Manner

Luciferase reporter assays were performed to further delineate a molecular basis for the transcriptional regulation of PPARα by ATF6. As shown in Fig. 5*A–D* and Supplementary Fig. 4, treatment with Ad-dnATF6 caused a significant reduction of PPARα-induced activation of the 3xPPRE luciferase reporter (32) in HEK293T cells and human Huh7 hepatocytes. Importantly, transfection of RXRα with PPARα resulted in a pronounced coactivation on the 3xPPRE reporter, which was strikingly abrogated by dnATF6. Moreover, dnATF6 blocked WY14643-stimulated induction of transcriptional activity of the 3xPPRE reporter. Consistently, knockdown of ATF6 by siRNAs resulted in a profound reduction of the transcriptional activity of PPARα in HepG2 cells. These data suggest that PPARα/RXRα heterodimer–mediated gene transcription requires ATF6. To further define whether hepatic ATF6 activity is physiologically relevant to PPARα activation in vivo, chromatin immunoprecipitation (ChIP) was performed in livers from HFHS diet–fed mice. Consistent with previous observations using electrophoretic mobility shift

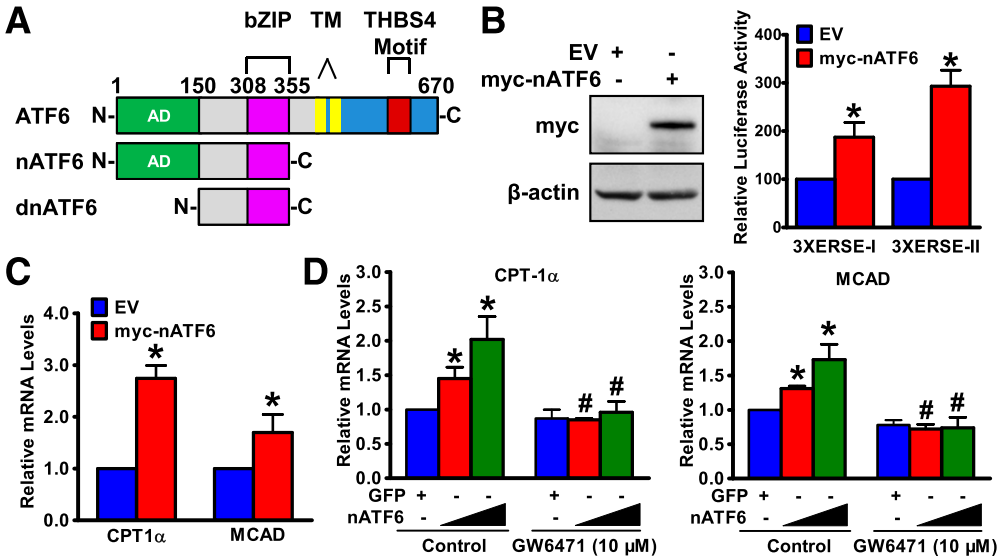

Figure 3—ATF6 stimulates hepatic fatty acid oxidation in a PPARα-dependent manner in hepatocytes. *A*: Schematic structures of full-length ATF6, nATF6, and dnATF6. *B*: nATF6 induces the transcriptional activity of ERSE-I and ERES-II reporter plasmids in HepG2 cells. Cells were cotransfected with the luciferase reporter plasmid encoding the ERSE-I or ERES-II element, along with *myc*-tagged nATF6 or empty vector (EV), and then cultured for 48 h. Overexpression of nATF6 in HEK293T cells was confirmed by immunoblots. *C*: nATF6 is sufficient to stimulate expression of genes involving fatty acid oxidation in HepG2 cells. Cells were transfected with the plasmid encoding nATF6 or EV, and then cultured for 48 h. *D*: The ability of an adenovirus encoding nATF6 to induce CPT1α and MCAD was abrogated by PPARα antagonist GW6471 in HepG2 cells. Cells were infected with Ad-GFP or Ad-nATF6 for 24 h, quiesced in serum-free DMEM overnight, and then treated for an additional 24 h with or without GW6471 (10 μmol/L). The data are represented as the mean ± SEM (n = 4–5). *P < 0.05 vs. EV or Ad-GFP together with control; #P < 0.05 vs. Ad-nATF6 and control.

assay (33), PPARα was recruited and bound to the two PPRE elements on the FGF21 promoter. As shown in Fig. 5*E*, PPARα binding to the FGF21 promoter was detected using primers extending from –1,039 to −936 and from –96 to −1, but not with primers that amplify a control distant region from –5,200 to –5,000. Strikingly, the occupancy of PPARα to the FGF21 promoter was abrogated by dnATF6.

In contrast, the active nATF6 potentiated WY14643-stimulated induction of transcriptional activity of the 3xPPRE reporter (Fig. 5*F*). As shown in Fig. 5*G*, the GST pull-down and immunoblotting analysis revealed that endogenous PPARα was detected in transfected and purified GST-tagged nATF6, suggesting that the active form of ATF6 binds to PPARα. Therefore, the data indicate that ATF6 may facilitate transcriptional activation of the PPARα through direct interaction, leading to improved hepatic lipid metabolism.

Hepatic Steatosis Is Exacerbated in Hepatic ATF6–Inhibited Mice During the Adaptive Fasting Response

To determine whether expression of ATF6 is regulated by nutritional status, expression levels of ATF6 in livers from fed or fasted mice were determined. ATF6 mRNA was strongly induced after 24 h of fasting (Fig. 6*A*), which is tightly correlated with fasting-induced expression of PPARα. Notably, mRNA levels of GRP78 and CHOP were not obviously changed. Body weight and liver weight were significantly reduced in mice by 24 h of fasting (Fig. 6*B–D*). Compared with the fed state, fasting caused induction of triglyceride levels and lipid deposition in mouse livers, which is consistent with our previous observation in mice (20). Strikingly, pronounced hepatic steatosis was observed in fasted mice treated with dnATF6, as evidenced by increased hepatic triglyceride levels and liver histologic analysis, suggesting that hepatic ATF6 is necessary for lipid metabolism under fasting condition. Notably, plasma triglyceride and liver and plasma cholesterol levels were similar between GFP- and dnATF6-treated mice at the fasting condition.

Moreover, the effects of hepatic ATF6 inhibition on hepatic PPARα signaling and fatty acid oxidation in mice were determined. Figure 6*E* and *F* show that dnATF6 caused a significant reduction of fasting-induced expression of PPARα targets such as MCAD, CPT1α, and FGF21. Compared with GFP-treated mice, a concerted reduction of serum FGF21 and β-hydroxybutyrate levels, an indicator of increased hepatic fatty acid oxidation and ketogenesis, was consistently observed in the fasted mice treated with dnATF6. Notably, the mRNA levels of lipogenic genes, including SREBP-1c, ACC1, and FAS, were not obviously changed by dnATF6 in fasted dnATF6-treated mice (Supplementary Fig. 5*A–C*), suggesting that de novo lipogenesis is not likely responsible for the exacerbated steatotic phenotypes in the fasted dnATF6-treated mice. Together, these data indicate that inhibition

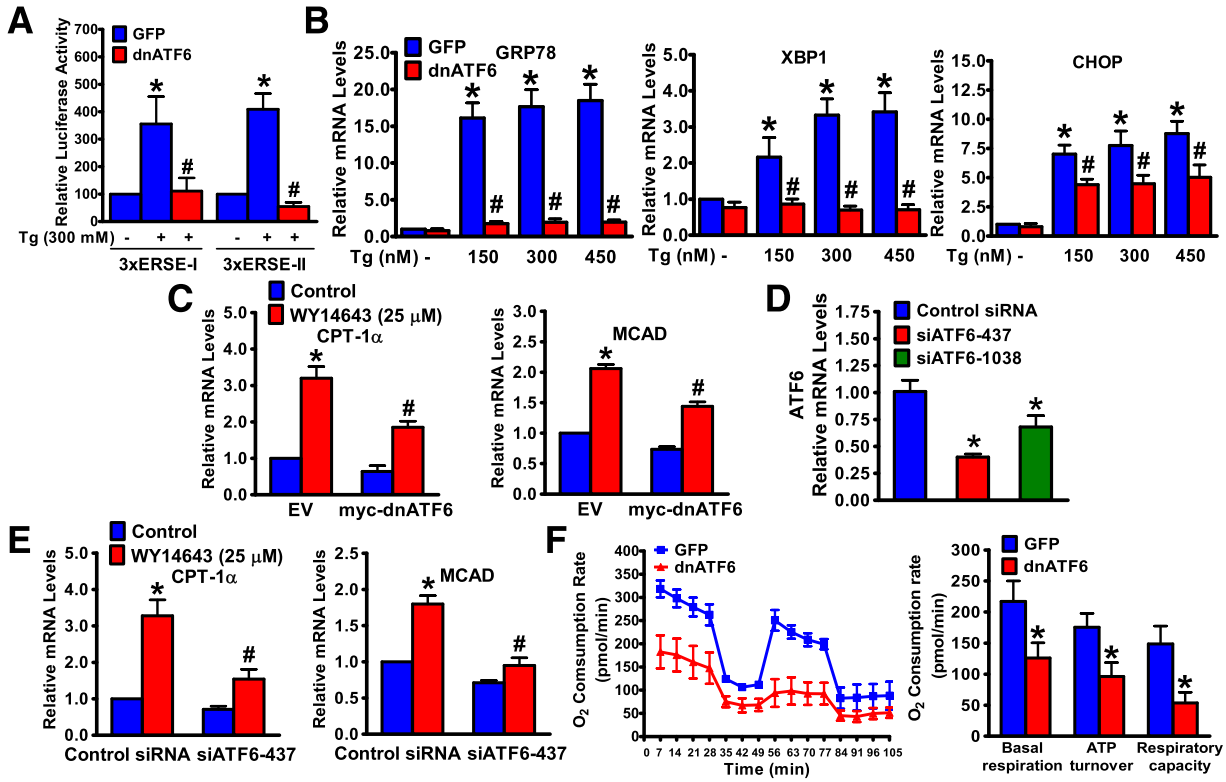

Figure 4—ATF6 is necessary for PPARα-induced mitochondrial fatty acid oxidation in hepatocytes. *A*: dnATF6 represses the transcriptional activity of ERSE-I and ERES-II reporter plasmids under ER stress conditions in HepG2 cells. *B*: dnATF6 inhibits thapsigargin (Tg)-induced expression of URP mediators in HepG2 cells. Cells were infected with Ad-GFP or Ad-dnATF6 for 48 h, followed by incubation, without or with Tg, overnight. ATF6 is required for PPARα agonist WY14643-induced mitochondria fatty acid oxidation in HepG2 cells. *C*: dnATF6 abrogates WY14643-stimulated fatty acid oxidation gene expression in HepG2 cells. *D* and *E*: WY14643-stimulated fatty acid oxidation gene expression is reduced by siRNA-mediated ATF6 knockdown in HepG2 cells. The mRNA amounts of ATF6 are decreased by ATF6 knockdown. Cells were transfected with empty vector (EV) pShuttle-CMV or pShuttle-*myc*-dnATF6 (*myc*-dnATF6), or control siRNA or siATF6 for 24 h, followed by incubation overnight in serum-free medium, and then treated without or with WY14643 (25 μmol/L) for 6 h. *F*: Inhibition of ATF6 represses the mitochondrial oxygen consumption rate in HepG2 cells. The oxygen consumption rates of basal respiration, ATP turnover, and respiratory capacity were measured and calculated as averages for each phase by Seahorse Bioscience extracellular flux analyzer. The data are represented as the mean ± SEM (n = 3–5). *P < 0.05 vs. EV, Ad-GFP, or control siRNA; #P < 0.05 vs. Ad-GFP and Tg or WY14643 together with EV or control siRNA.

of ATF6 in the liver suppresses hepatic fatty acid oxidation and leads to exacerbated hepatic steatosis during adaptive fasting response.

Adenovirus-Mediated Overexpression of the Active Form of ATF6 Protects Against Hepatic Steatosis in HFHS Diet–Fed Mice

Given that diet- and fasting-induced hepatic steatosis is associated with attenuated transcriptional activity of the ATF6-PPARα complex in the liver (Figs. 1 and 6), the actions of ATF6 gain-of-function on the steatotic phenotypes in mouse livers were determined. Remarkably, hepatic steatosis in mice fed the HFHS diet was improved by adenovirus-mediated overexpression of active form of ATF6 (Ad-nATF6), which was evidenced by reduced liver triglyceride levels and by H&E and Oil Red O staining showing decreased hepatic fat deposition (Fig. 7*A–C*). Notably, body weight and lean and fat mass were not obviously changed (Supplementary Fig. 6*A* and *B*). Moreover, Ad-nATF6 improved HFHS diet–caused glucose intolerance and insulin resistance, as evidenced by reduced fasting blood glucose, plasma insulin levels, and homeostasis model assessment of insulin resistance (Fig. 7*D* and Supplementary Fig. 6*C*).

Next, we further determined whether induction of PPARα signaling and hepatic fatty acid oxidation is responsible for improved steatotic phenotypes in Ad-nATF6–treated mice. The expression of nATF6 in the liver was evidenced by RT-PCR (Fig. 7*E* and *F*). Gene expression levels of UPR mediators, such as GRP78 and CHOP, as well as PPARα downstream targets, such as MCAD and CPT1α, were largely increased by treatment with Ad-nATF6. Consequently, plasma β-hydroxybutyrate levels were increased by Ad-nATF6 (Fig. 7*G*). These results strongly suggest that activation of PPARα and hepatic fatty acid oxidation are indeed responsible for improved hepatic steatosis in the hepatic nATF6-overexpressed mice.

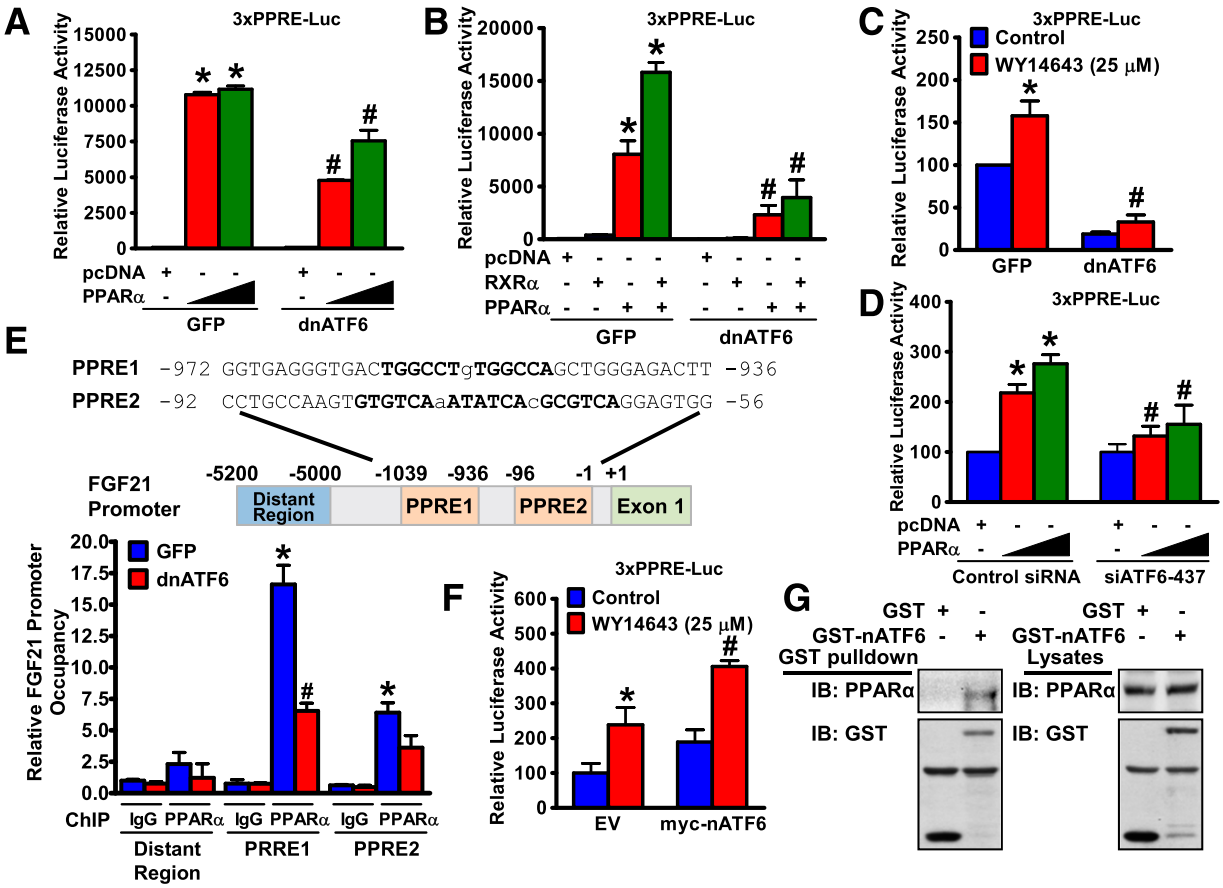

Figure 5—ATF6 is required for the transcriptional activity of PPARα. Inhibition or siRNA-mediated knockdown of ATF6 reduces the transcriptional activity of PPARα. *A*: PPARα-stimulated induction of transcriptional activity of the 3xPPRE reporter is abrogated by dnATF6. The black triangle bar indicates increased doses of PPARα plasmid (0.2 μg and 0.5 μg). *B*: Coactivation of PPARα and RXRα heterodimer on the transcriptional activity of the 3xPPRE reporter is diminished by inhibition of ATF6. *C*: ATF6 is required for WY14643-induced transcriptional activity of the 3xPPRE reporter. *D*: siRNA-mediated knockdown of ATF6 attenuates the transcriptional activity of PPARα in HepG2 cells. The data are represented as the mean ± SEM (n = 3–5). *P < 0.05 vs. pcDNA or control; #P < 0.05 vs. PPARα, PPARα and RXRα, or WY14643. *E*: The occupancy of endogenous PPARα on the FGF21 promoter is abrogated by inhibition of ATF6 in mouse livers. In vivo quantitative ChIP assays were performed using PPARα antibody or control antibody against IgG. The specificity of the ChIP signal at the FGF21 loci was confirmed by minimal binding that occurred in the distal upstream region or with IgG immunoprecipitation. The value obtained from Ad-GFP mice with IgG immunoprecipitation was set to 1, and fold-enrichment relative to this value was presented as the mean ± SEM (n = 5–6). *P < 0.05 vs. GFP mice with IgG immunoprecipitation in the specific PPRE site; #P < 0.05 vs. GFP mice with PPARα immunoprecipitation in the specific PPRE site. Two PPRE-like sequences are located in the mouse FGF21 promoter. The PPRE-like sequences are in boldface type. *F*: Overexpression of ATF6 potentiates WY14643-induced transcriptional activity of the 3xPPRE reporter in HepG2 cells (n = 3–4). *G*: The active form of ATF6 physically associates with endogenous PPARα in HEK293T cells. Cells were transfected with the plasmid encoding GST-nATF6 or GST control and then cultured for 48 h, followed by GST pull-down analysis. IB, immunoblot.

DISCUSSION

The UPR, a pathway in response to accumulation of misfolded proteins in the ER, has been implicated in a variety of diseases, including metabolic disease (34). Although the detrimental effects of ER stress in metabolic disease have been extensively studied, metabolic function and the underlying mechanism by which the UPR mediators affect the regulation of glucose and lipid metabolism are still poorly understood. In this report, we identify the key ER quality control protein, ATF6, as an important regulator of hepatic fatty acid oxidation. Mechanistically, we demonstrate that ATF6 stimulates hepatic fatty acid oxidation by direct interaction with PPARα. ATF6-mediated activation of PPARα may represent an alternative avenue to improve liver function and treat hepatic steatosis in obesity.

Regulation of PPARα by ATF6 in the Liver

The current study uses in vivo and in vitro approaches to demonstrate a novel regulation between the key UPR sensor ATF6 and PPARα. Several lines of evidence link ATF6 to the PPARα pathway. First, expression levels of hepatic ATF6 are induced by prolonged fasting, which is correlated with increased expression of PPARα (35). Second, ATF6 directly regulates the activity of PGC1α (9), a key transcription cofactor to activate PPARα (36). Third, ATF6-deficient mice are prone to develop tunicamycin-induced

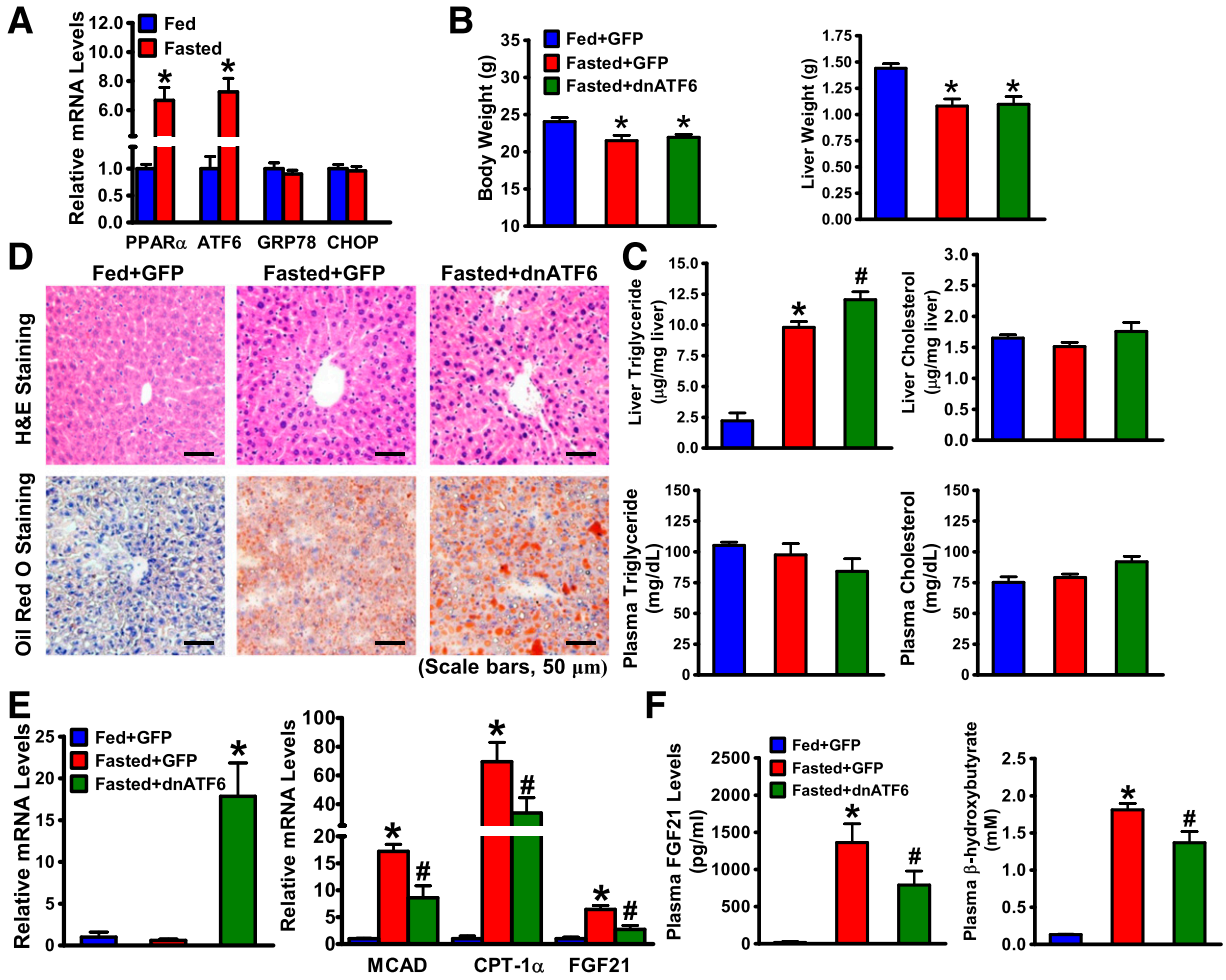

Figure 6—Hepatic inhibition of ATF6 increases susceptibility to developing fasting-induced hepatic steatosis. Male C57BL/6 mice (8 weeks old) were treated with Ad-GFP or Ad-dnATF6 adenoviruses via tail vein injection for 1 week and then were fed or fasted for 24 h. *A*: Expression of hepatic ATF6 is increased in response to nutrient deprivation in mice. The mRNA amounts of genes encoding PPARα, ATF6, GRP78, and CHOP in the mouse livers were determined by real-time PCR. *B*: Effects of fasting on body weight and liver weight in mice. *C*: Triglyceride and cholesterol levels in the liver or plasma were assessed. *D*: Representative H&E and Oil Red O staining are shown (scale bars: 50 μm). *E*: Fasting-induced hepatic fat oxidation gene expression was attenuated by dnATF6 in mice. mRNAs of overexpressed dnATF6 and hepatic CPT1α, MCAD, and FGF21 were determined by real-time PCR. *F*: Plasma levels of FGF21 and β-hydroxybutyrate in mice. The data are represented as the mean ± SEM (n = 4–7). *P < 0.05 vs. fed mice treated with Ad-GFP; #P < 0.05 vs. fasted mice treated with Ad-GFP.

hepatic steatosis, which is associated with decreased expression of PPARα (14,15). Moreover, the current study shows that the transcriptional activity of genetic or pharmaceutic manipulation of PPARα is significantly impaired in ATF6 inhibition or knockdown hepatocytes, whereas increased ATF6 activity enhances PPARα activity. Given that ATF6 deficiency in other tissues is likely to systemically affect hepatic lipid metabolism in the whole-body ATF6-KO mice, the current study uses adenovirus-mediated hepatic overexpression of dnATF6 and identifies a direct link between ATF6 and PPARα. At the molecular level, ATF6 inhibition represses the recruitment of PPARα to the target gene promoter containing the PPRE element. Furthermore, our data suggest that ATF6 is required for PPARα signaling primarily through the activation of PPARα/RXRα. Given that coactivation of ATF6 with PGC1α was known to regulate skeletal muscle function (36), future studies should reveal whether ATF6 promotes induction of PPARα signaling through PGC1α in the liver.

ATF6 Enhances the Activity of PPARα to Increase Hepatic Fatty Acid Oxidation and Attenuate Hepatic Steatosis in Mice

One of the major findings of the current study is that hepatic inhibition of ATF6 increases the susceptibility to develop hepatic steatosis in mice, particularly in conditions of diet-induced obesity and during the adaptive starvation response. This study demonstrates that steatosis caused by inhibition of ATF6 activity is at least partly attributed to a reduction of PPARα signaling and hepatic fatty acid oxidation. Moreover, this study identifies

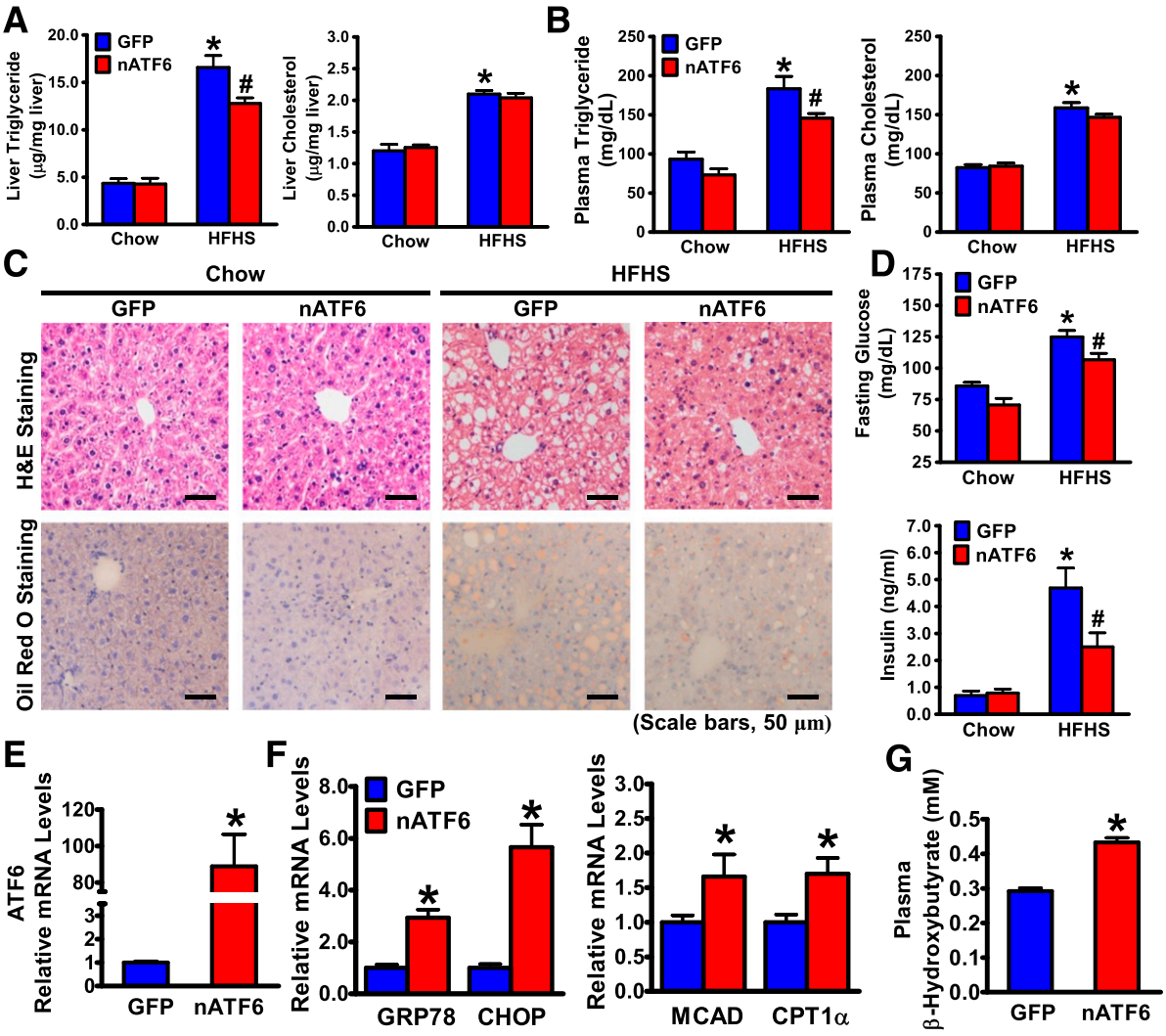

Figure 7—Hepatic overexpression of the active form of ATF6 stimulates hepatic fatty acid oxidation to attenuate hepatic steatosis in HFHS diet-fed mice. Male C57BL/6 mice (8 weeks old) were fed a chow diet for 4 weeks or an HFHS diet for 12 weeks, followed by treatment with Ad-GFP or Ad-dnATF6 via tail vein injection for 2 weeks. Adenovirus-mediated overexpression of nATF6 decreases hepatic steatosis in HFHS diet-fed mice. Liver (*A*) and plasma (*B*) triglyceride and cholesterol levels were assessed in mice. *C*: Representative H&E and Oil Red O staining is shown (scale bars: 50 μm). *D*: Blood glucose and plasma insulin levels were assessed. *E*: Hepatic gene expression of nATF6 in mice fed the HFHS diet. *F*: Hepatic overexpression of ATF6 stimulates gene mRNA levels of UPR mediators and fatty acid oxidation genes in livers of HFHS diet–fed mice. Hepatic gene expression was determined by real-time PCR. *G*: Plasma levels of β-hydroxybutyrate in HFHS diet–fed mice. The data are represented as the mean ± SEM (n = 5–7). *P < 0.05 vs. chow and Ad-GFP; #P < 0.05 vs. HFHS and Ad-GFP.

that ATF6 interacts with PPARα to control hepatic lipid homeostasis. Importantly, in vivo ChIP assays provide biochemical evidence that the binding ability of PPARα to the PPRE site of the target gene promoter is attenuated by ATF6 inhibition, suggesting that ATF6 plays a critical role in PPARα signaling.

In contrast, activation of ATF6 by overexpression of the active form of ATF6 enhances PPARα activity and protects against hepatic steatosis. These data support the essential role of ATF6 in mediating hepatic lipid metabolism and also indicate that the steatotic phenotype observed in dnATF6-treated mice is unlikely caused by off-target effects caused by adenovirus-mediated gene transfer. This study establishes that the UPR modulates fatty acid metabolism in response to nutrient overload, suggesting a cross talk between the UPR and nuclear receptor coordinates at the transcriptional level and contributes to hepatic lipid homeostasis.

The UPR Protects Against Hepatic Steatosis in Response to ER Stress

The three major UPR pathways have been implicated in the regulation of lipid metabolism (37). Rutkowski et al. (14) hypothesized that in addition to the CHOP-C/EBPα axis, other as-yet unknown mechanisms are responsible for hepatic fat oxidation and lipid homeostasis in

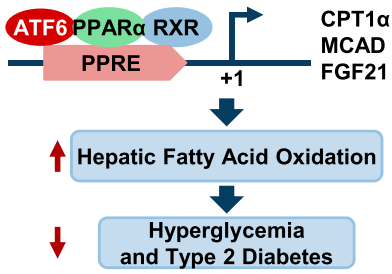

Figure 8—The proposed model for hepatic ATF6 as a novel regulator of PPARα. ATF6 stimulates hepatic fatty acid oxidation possibly through interaction with PPARα. The PPARα/RXR heterodimer may serve as the key functional regulator transducing ATF6 signaling to the transcription of genes involving hepatic fatty acid oxidation, such as CPT1α, MCAD, and FGF21, via the PPRE sequence. Improved hepatic lipid metabolism may result in enhanced systemic glucose homeostasis possibly through increased hepatic β-oxidation and/or some endocrine effects of FGF21. The cross talk between the UPR and nuclear receptor may coordinate at the transcriptional level and contribute to lipid and glucose homeostasis.

response to ER stress. The current study is the first to use gain- and loss-of-function approaches to demonstrate that ATF6 is sufficient and necessary for hepatic steatosis in mice in response to nutrient overload and fasting treatment. The ATF6-PPARα axis appears to protect against excessive increases in hepatic lipid accumulation, whereas deregulation of this signaling leads to hepatic steatosis (Fig. 8). Interestingly, ATF6 activity was decreased in livers of high fat diet–induced obese mice and in genetically obese *ob/ob* mice (8). These findings are also consistent with exacerbation of hepatic steatosis by the deficiency of ATF6 or ER quality control gene $p58^{IPK}$ in tunicamycin-treated mice (14,15) or improvement of hepatic steatosis by overexpression of ER chaperone GRP78 in *ob/ob* mice (38). This study supports the notion that initial ER stress–caused activation of the adaptation and/or recovery UPR pathways, such as ATF6, restores lipid dysregulation and maintains metabolic homeostasis, whereas persistently severe ER stress results in exacerbated metabolic dysfunction, possibly through the antiadaptive CHOP activation (14).

In conclusion, we have shown that PPARα is a major target of ATF6 in the liver to regulate fatty acid oxidation and control lipid homeostasis. These findings provide a novel mechanism by which ATF6 regulates lipid and glucose metabolism and suggest that therapeutic strategies designed to modulate ATF6 may be beneficial for the treatment of hepatic steatosis as well as insulin resistance in the obesity condition.

Acknowledgments. The authors thank Dr. Ray Lu (University of Guelph) for providing ERSE-I and ERSE-II luciferase reporters, Dr. Feng Liu (University of Texas Health Science Center at San Antonio) for helpful discussion, Yi Yang (Niumag) for body composition analysis, and Yuehong Yang and Zhonghui Weng (Institute for Nutritional Sciences) for technical assistance.

Funding. This work has been supported by grants from the National Natural Science Foundation of China (nos. 81270930 and 31471129) and the Hundred Talents Program of the Chinese Academy of Sciences (2013OHTP04) to Y. Li.

Duality of Interest. No potential conflicts of interest relevant to this article were reported.

Author Contributions. X.C. and Y. Li contributed to experiment design and wrote the manuscript. X.C., F.Z., Q.G., A.C., S.Z., Z.H., Y.H., J.G., Y.S., and Z.L. contributed to the acquisition and analysis of data. Y.Le provided reagents and material support. Z.Y., L.Q.D., Xia.G., and Xin.G. reviewed the manuscript. Y. Li obtained the funding. Y. Li is the guarantor of this work and, as such, had full access to all the data in the study and takes responsibility for the integrity of the data and the accuracy of the data analysis.

Prior Presentation. Parts of this study were presented in abstract form at the 75th Scientific Sessions of the American Diabetes Association, Boston, MA, 5–9 June 2015.

References

1. McGarry JD, Foster DW. Regulation of hepatic fatty acid oxidation and ketone body production. Annu Rev Biochem 1980;49:395–420
2. Cohen JC, Horton JD, Hobbs HH. Human fatty liver disease: old questions and new insights. Science 2011;332:1519–1523
3. Rutkowski DT, Kaufman RJ. A trip to the ER: coping with stress. Trends Cell Biol 2004;14:20–28
4. Schröder M, Kaufman RJ. The mammalian unfolded protein response. Annu Rev Biochem 2005;74:739–789
5. Özcan U, Cao Q, Yilmaz E, et al. Endoplasmic reticulum stress links obesity, insulin action, and type 2 diabetes. Science 2004;306:457–461
6. Fu S, Watkins SM, Hotamisligil GS. The role of endoplasmic reticulum in hepatic lipid homeostasis and stress signaling. Cell Metab 2012;15:623–634
7. Yamamoto K, Sato T, Matsui T, et al. Transcriptional induction of mammalian ER quality control proteins is mediated by single or combined action of ATF6α and XBP1. Dev Cell 2007;13:365–376
8. Wang Y, Vera L, Fischer WH, Montminy M. The CREB coactivator CRTC2 links hepatic ER stress and fasting gluconeogenesis. Nature 2009;460:534–537
9. Wu J, Ruas JL, Estall JL, et al. The unfolded protein response mediates adaptation to exercise in skeletal muscle through a PGC-1α/ATF6α complex. Cell Metab 2011;13:160–169
10. Lynch JM, Maillet M, Vanhoutte D, et al. A thrombospondin-dependent pathway for a protective ER stress response. Cell 2012;149:1257–1268
11. Karali E, Bellou S, Stellas D, Klinakis A, Murphy C, Fotsis T. VEGF Signals through ATF6 and PERK to promote endothelial cell survival and angiogenesis in the absence of ER stress. Mol Cell 2014;54:559–572
12. Zhou Y, Lee J, Reno CM, et al. Regulation of glucose homeostasis through a XBP-1-FoxO1 interaction. Nat Med 2011;17:356–365
13. Usui M, Yamaguchi S, Tanji Y, et al. Atf6α-null mice are glucose intolerant due to pancreatic β-cell failure on a high-fat diet but partially resistant to diet-induced insulin resistance. Metabolism 2012;61:1118–1128
14. Rutkowski DT, Wu J, Back S-H, et al. UPR pathways combine to prevent hepatic steatosis caused by ER stress-mediated suppression of transcriptional master regulators. Dev Cell 2008;15:829–840
15. Yamamoto K, Takahara K, Oyadomari S, et al. Induction of liver steatosis and lipid droplet formation in ATF6α-knockout mice burdened with pharmacological endoplasmic reticulum stress. Mol Biol Cell 2010;21:2975–2986
16. Shulman AI, Mangelsdorf DJ. Retinoid x receptor heterodimers in the metabolic syndrome. N Engl J Med 2005;353:604–615
17. Leone TC, Weinheimer CJ, Kelly DP. A critical role for the peroxisome proliferator-activated receptor α (PPARalpha) in the cellular fasting response: the PPARalpha-null mouse as a model of fatty acid oxidation disorders. Proc Natl Acad Sci U S A 1999;96:7473–7478
18. Li Y, Xu S, Mihaylova MM, et al. AMPK phosphorylates and inhibits SREBP activity to attenuate hepatic steatosis and atherosclerosis in diet-induced insulin-resistant mice. Cell Metab 2011;13:376–388

19. Li Y, Xu S, Jiang B, Cohen RA, Zang M. Activation of sterol regulatory element binding protein and NLRP3 inflammasome in atherosclerotic lesion development in diabetic pigs. PLoS One 2013;8:e67532
20. Li Y, Wong K, Giles A, et al. Hepatic SIRT1 attenuates hepatic steatosis and controls energy balance in mice by inducing fibroblast growth factor 21. Gastroenterology 2014;146:539–549.e7
21. Yoshida H, Okada T, Haze K, et al. ATF6 activated by proteolysis binds in the presence of NF-Y (CBF) directly to the cis-acting element responsible for the mammalian unfolded protein response. Mol Cell Biol 2000;20:6755–6767
22. Tontonoz P, Hu E, Graves RA, Budavari AI, Spiegelman BM. mPPAR gamma 2: tissue-specific regulator of an adipocyte enhancer. Genes Dev 1994;8:1224–1234
23. Gong Q, Hu Z, Zhang F, et al. Fibroblast growth factor 21 improves hepatic insulin sensitivity by inhibiting mammalian target of rapamycin complex 1. Hepatology. 29 February 2016 [Epub ahead of print]. DOI: 10.1002/hep.28523
24. Li Y, Wong K, Walsh K, Gao B, Zang M. Retinoic acid receptor β stimulates hepatic induction of fibroblast growth factor 21 to promote fatty acid oxidation and control whole-body energy homeostasis in mice. J Biol Chem 2013;288:10490–10504
25. Li Y, Xu S, Giles A, et al. Hepatic overexpression of SIRT1 in mice attenuates endoplasmic reticulum stress and insulin resistance in the liver. FASEB J 2011;25:1664–1679
26. Yoshida H, Matsui T, Yamamoto A, Okada T, Mori K. XBP1 mRNA is induced by ATF6 and spliced by IRE1 in response to ER stress to produce a highly active transcription factor. Cell 2001;107:881–891
27. Purushotham A, Schug TT, Xu Q, Surapureddi S, Guo X, Li X. Hepatocyte-specific deletion of SIRT1 alters fatty acid metabolism and results in hepatic steatosis and inflammation. Cell Metab 2009;9:327–338
28. Zeng L, Lu M, Mori K, et al. ATF6 modulates SREBP2-mediated lipogenesis. EMBO J 2004;23:950–958
29. Yamamoto K, Yoshida H, Kokame K, Kaufman RJ, Mori K. Differential contributions of ATF6 and XBP1 to the activation of endoplasmic reticulum stress-responsive cis-acting elements ERSE, UPRE and ERSE-II. J Biochem 2004;136:343–350
30. Xu HE, Stanley TB, Montana VG, et al. Structural basis for antagonist-mediated recruitment of nuclear co-repressors by PPARalpha. Nature 2002;415:813–817
31. Takao K, Noguchi K, Hashimoto Y, Shirahata A, Sugita Y. Synthesis and evaluation of fatty acid amides on the N-oleoylethanolamide-like activation of peroxisome proliferator activated receptor α. Chem Pharm Bull (Tokyo) 2015;63:278–285
32. Kim JB, Wright HM, Wright M, Spiegelman BM. ADD1/SREBP1 activates PPARgamma through the production of endogenous ligand. Proc Natl Acad Sci U S A 1998;95:4333–4337
33. Inagaki T, Dutchak P, Zhao G, et al. Endocrine regulation of the fasting response by PPARalpha-mediated induction of fibroblast growth factor 21. Cell Metab 2007;5:415–425
34. Wang S, Kaufman RJ. The impact of the unfolded protein response on human disease. J Cell Biol 2012;197:857–867
35. Kersten S, Seydoux J, Peters JM, Gonzalez FJ, Desvergne B, Wahli W. Peroxisome proliferator-activated receptor α mediates the adaptive response to fasting. J Clin Invest 1999;103:1489–1498
36. Vega RB, Huss JM, Kelly DP. The coactivator PGC-1 cooperates with peroxisome proliferator-activated receptor α in transcriptional control of nuclear genes encoding mitochondrial fatty acid oxidation enzymes. Mol Cell Biol 2000;20:1868–1876
37. Hotamisligil GS. Endoplasmic reticulum stress and the inflammatory basis of metabolic disease. Cell 2010;140:900–917
38. Kammoun HL, Chabanon H, Hainault I, et al. GRP78 expression inhibits insulin and ER stress-induced SREBP-1c activation and reduces hepatic steatosis in mice. J Clin Invest 2009;119:1201–1215